Headgroup structure and cation binding in phosphatidylserine lipid bilayers

Hanne Antila,[†] Pavel Buslaev,[‡] Fernando Favela-Rosales,[¶] Tiago M. Ferreira,[§] Ivan Gushchin,[‡] Matti Javanainen,[‖] Batuhan Kav,[†] Jesper J. Madsen,[⊥] Josef Melcr,[‖] Markus Miettinen,[†] Ricky Nencini,[‖] O. H. Samuli Ollila,[*,‖] and Thomas J. Piggot[△]

†*Department of Theory and Bio-Systems, Max Planck Institute of Colloids and Interfaces, 14424 Potsdam, Germany*

‡*Moscow Institute of Physics and Technology, Dolgoprudny, Russia*

¶*Departamento de Investigación, Tecnológico Nacional de México, Campus Zacatecas Occidente, México*

§*NMR group - Institute for Physics, Martin-Luther University Halle-Wittenberg*

‖*Institute of Organic Chemistry and Biochemistry of the Czech Academy of Sciences, Flemingovo nám. 542/2, CZ-16610 Prague 6, Czech Republic*

⊥*Department of Chemistry, The University of Chicago, Chicago, Illinois, United States of America*

#*Department of Global Health, College of Public Health, University of South Florida, Tampa, Florida, United States of America*

@*Institute of Biotechnology, University of Helsinki*

△*Chemistry, University of Southampton, Highfield, Southampton SO17 1BJ, U.K*

E-mail: samuli.ollila@helsinki.fi

Abstract

Phosphatidylserine (PS) is a negatively charged lipid commonly found in eukaryotic membranes, where it interacts with proteins via nonspecific electrostatic interactions as well as via specific binding. Moreover, in the presence of calcium ions, PS can induce membrane fusion and phase separation. Molecular details of these phenomena remain poorly understood, partly because accurate models to interpret the experimental data have not been available. Here we gather a set of experimental NMR data of C–H bond order parameter magnitudes, $|S_{\mathrm{CH}}|$, for pure PS and mixed PS:PC (phosphatidylcholine) lipid bilayers, and augment this data set by measuring the signs of S_{CH} in the POPS headgroup using S-DROSS solid-state NMR spectrsocopy. This data set is then used to assess the accuracy of 1) the PS headgroup structures and 2) the ion binding to PS-containing membranes in the most commonly used classical molecular dynamics (MD) models including CHARMM36, Lipid17, Macrog, Slipids, GROMOS-CKP, Berger and variants. We show large discrepancies between different force-fields and that none of the models reproduces the NMR data within experimental accuracy. However, the best MD models can detect the most essential differences between PC and PS headgroup structures. In line with our previous results for PC lipids, none of the PS force fields correctly captures the cation binding affinity. Moreover, the response of PS headgroups to bound ions can differ from experiments even *qualitatively*. The collected experimental dataset and simulation results pave the way for the improvement of lipid force fields that correctly describe the biologically relevant negatively charged membranes and their interactions with ions. This work is part of the NMRlipids open collaboration project (`nmrlipids.blogspot.fi`).

Introduction

Phosphatidylserine (PS) is the most common negatively charged lipid type in eukaryotic biomembranes. In red blood cells, for example, PS lipids compose 8.5% of the total lipid weight.[1] The abundance, however, varies between different cells and organelles, and up to

25–35% of the cytosolic leaflet of plasma membranes consists of PS lipids.[2,3] PS lipids are vastly important biomolecules that interact with signaling proteins,[2] regulate surface charge and protein localization,[4] and induce protein aggregation.[5,6] Some protein domains interact specifically with PS lipids, while other protein sites attract PS lipids by nonspecific electrostatics and the binding can be regulated by calcium.[2] Therefore, deciphering the structural details of lipid headgroups and the details of cation binding is crucial for understanding PS-mediated processes on cellular membranes.

Experimental studies have indicated that the serine headgroup in PS is more rigid than the choline headgroup in phosphatidylcholine (PC), owing possibly to electrostatic interactions or formation of a hydrogen bond network between the headgroups.[7,8] While most monovalent ions interact weakly with PS-containing bilayers, multivalent cations and Li^+ are able to form strong dehydrated molecular complexes with PS lipids.[9–19] The dehydrated complexes of PS headgroups with calcium ions can even lead to phase separation.[9,10,14–18] Mixing PS lipids with PC lipids reduces their propensity to form strong complexes with multivalent ions and makes the PS headgroup less rigid.[7,8,17,18] That being said, some studies suggest that Ca^{2+} has similar specific binding affinity to both negatively charged and zwitterionic phospholipids, and that the increased cation binding to PS lipid bilayers is non-specific and arises only due to the increased local cation concentration in the vicinity of the membrane.[20,21]

Molecular level interpretations of the rigidity of PS headgroup and its interactions with ions are currently lacking. Classical molecular dynamics (MD) simulations have been widely used in efforts to understand the PS headgroup structure, its influence on lipid bilayer properties, and its interaction with ions.[19,22–34] Unfortunately, the results have depended on the particular force field used. For example, recent simulations using the NBfix parameters for Ca^{2+}[35] in the CHARMM36 force field,[29,36] combined with 2D infrared spectroscopy, suggest that calcium ions interact only with the carboxylate group of PS lipids.[33] In contrast, the results from the same lipid model without the NBfix ion parameters, combined with NMR chemical shifts and rotational-echo double-resonance (REDOR) experiments, indicate

a significant binding affinity also toward the phosphate region.[34] Meanwhile, simulations with the Berger force field,[24,37] combined with fluorescent and vibrational sum frequency spectroscopy, suggest substantial calcium binding to the carbonyls in the acyl chains.[32]

We have recently demonstrated that the lipid C–H bond order parameters, S_{CH}, can be used to resolve such controversies.[38,39] The S_{CH} can be measured from NMR experiments with high accuracy and directly compared to simulations to either evaluate the quality of the simulation model and/or to interpret the experiments.[40] Using this approach, it has been established that the structure of PC lipid headgroup and glycerol backbone are not well captured by most MD force fields,[38] that the cation binding to PC lipid bilayers is overestimated,[39] and that the inequivalent order parameters of the distinct C–H bonds at carbon 2 in *sn*-2 lipid tails is correctly reproduced only in the CHARMM36 force field.[41]

Here, we first extend the available set of experimentally measured PS lipid headgroup and glycerol backbone C–H bond order parameters by measuring the signs of these order parameters using S-DROSS solid-state NMR spectroscopy. Based on the collected experimental data, we then assess the quality of headgroup structures and the ion binding affinity in the available MD simulation models of PS lipids. Our results pave the way for the development of lipid models that correctly describe the headgroup region of negatively charged lipids under physiological salt conditions. Such force fields are expected to be extremely useful in understanding the biological functions of lipid headgroups and glycerol backbone, as these are known to behave similarly in simple model membranes and in cells.[20,42,43]

Methods

Experimental C–H bond order parameters

The magnitudes of headgroup and glycerol backbone C–H bond order parameters of 1-palmitoyl-2-oleoyl-*sn*-glycero-3-phospho-L-serine (POPS) were determined by measuring the chemical-shift resolved dipolar splittings with a R-type Proton Detected Local Field

(R-PDLF) experiment.[44] The corresponding order parameter signs were measured with a S-DROSS experiment[45] using natural abundance ^{13}C solid state NMR spectroscopy as described previously.[46,47] The experiments were done in a Bruker Avance III 400 spectrometer operating at a ^{1}H Larmor frequency of 400.03 MHz. Magic angle spinning (MAS) of the sample was used at a frequency of 5.15 kHz (R-PDLF) and 5 kHz (S-DROSS). The following experimental setups were used.

C–H bond order parameters from the R-PDLF experiment. The parameters are described according to Figures 1c and 2c of the original reference for the R-PDLF experiment.[44] The refocused-INEPT delays were $\tau_1 = 1.94$ ms and $\tau_2 = 0.97$ ms. The used radio frequency pulses had the following nutation frequencies: 46.35 kHz ($R18_1^7$ pulses), 63.45 kHz (^{13}C 90° and 180°), 50 kHz (SPINAL64 ^{1}H decoupling pulses). The t_1 increment was equal to 10.79 μs $\times 18 \times 2$, and 32 points in the indirect dimension were recorded using 1024 scans for each, with a recycle delay of 5 s and a spectral width of 149.5 ppm.

Order parameter signs from the S-DROSS experiment. The parameters are described according to Figures 1b and 1c of the original reference for the S-DROSS experiment.[45] The refocused-INEPT delay δ_2 was 1.19 ms. The τ_1 and τ_2 in the S-DROSS recoupling blocks R were set as $\tau_1 = 39.4$ μs and $\tau_2 = 89.4$ μs. The used radio frequency pulses had the nutation frequencies: 63.45 kHz (^{13}C 90° and 180°), 50 kHz (^{1}H SPINAL64 decoupling). The t_1 increment (dipolar recoupling dimension) was 800 μs, and a total of 8 points along t_1 were measured using 1024 scans for each, with a recycle delay of 5 s and a spectral width of 149.5 ppm.

Numerical simulations of S-DROSS curves. The numerical simulations of S-DROSS curves were performed using the SIMPSON simulation package[48] by inputing the ^{13}C–^{1}H dipolar couplings, either as determined by the R-PDLF experiments, or as calculated from the known ^{2}H quadrupolar couplings.[7] The chemical shift anisotropy and homonuclear couplings were neglected, and the SIMPSON input file *rep2000* was used to simulate a random distribution of bilayer orientations in the samples studied.

Sample preparation. The sample was prepared simply by mixing POPS powder (1-palmitoyl-2-oleoyl-*sn*-glycero-3-phospho-L-serine, purchased from Avanti Polar Lipids as sodium salt) with water (lipid:water 60:40 wt-%) in an Eppendorf tube, centrifuging the mixture and stirring with a thin glass rod repeatedly (approximately 5 to 6 times centrifuging/stirring) until a homogeneous viscous fluid was visually observed. Then 20 mg of the sample was transferred to an NMR insert suitable for 4 mm NMR rotors.

Molecular dynamics simulations

Molecular dynamics simulation data were collected using the Open Collaboration method,[38] with the NMRlipids Project blog (`nmrlipids.blogspot.fi`) and GitHub repository (`github.com/NMRlipids/NMRlipidsIVotherHGs`) as the communication platforms. The simulated systems are listed in Tables 1 (pure PS bilayers without additional ions) and 2 (mixed PC:PS bilayers at various salt concentrations). Further simulation details are given in the SI, and the simulation data are indexed in a searchable database available at `www.nmrlipids.fi`, and in the NMRlipids/MATCH repository (`github.com/NMRlipids/MATCH`).

The C–H bond order parameters were calculated directly from the carbon and hydrogen positions using the definition

$$S_{\mathrm{CH}} = \frac{1}{2}\langle 3\cos^2\theta - 1\rangle, \tag{1}$$

where θ is the angle between the C–H bond and the membrane normal (taken to align with z, with bilayer periodicity in the xy-plane). Angular brackets denote average over all sampled configurations. The order parameters were calculated by first averaging over time separately for each lipid in the system, and then calculating the average and the standard error of the mean over the different lipids. The analysis can be conducted using a Python program (`calcOrderParameters.py`, available in Ref. 101) that uses the MDAnalysis library.[102,103] For united atom models, the positions of hydrogens were generated before the order parameter calculation using the `protonate` tool of the Gromacs 3 sofware package.[104]

Table 1: List of MD simulations of pure PS bilayers without additional salt. Notation 2×[time] indicates that two independent MD runs were conducted. JC refers to the Joung–Cheatham ion parameters[49] and ff99 to the default Amber ion parameters.[50] Additional simulation details are given in the supplementary information. * Force field parameters for PS lipids generated for this work, for full details see the supplementary information.

lipid/counter-ions	force field	[a]N_l	[b]N_w	[c]T (K)	[d]t_{sim}(ns)	[e]t_{anal} (ns)	[f]files
POPS/Na^+	CHARMM36[29]	128	4480	298	2×500	2×100	51
POPS/K^+	CHARMM36[29]	128	4480	298	2×500	2×100	52
POPS/Na^+	CHARMM36-UA*[29,53]	128	4480	298	2×500	2×100	54
POPS/Na^+	MacRog[55]	128	4480	298	2×500	2×100	56
POPS/K^+	MacRog[55]	128	4480	298	200	150	57
POPS/Na^+	Lipid17[58] / JC[49]	128	4480	298	2×600	2×100	59
POPS/Na^+	Lipid17[58] / ff99[50]	128	4480	298	2×600	2×100	60
POPS/Na^+	Berger[24]	128	4480	298	2×500	2×100	61
POPS/Na^+	GROMOS-CKPM[62–64]	128	4480	298	2×500	2×100	65
POPS/Na^+	GROMOS-CKP[62–64]	128	4480	298	2×500	2×100	66
POPS/Na^+	Slipids[67]	128	4480	298	2×500	2×100	68
DOPS/Na^+	CHARMM36[29]	128	4480	303	2×500	2×100	69
DOPS/Na^+	CHARMM36-UA*[29,53]	128	4480	303	2×500	2×100	70
DOPS/Na^+	Lipid17[58] / JC[49]	128	4480	303	2×600	2×100	71
DOPS/Na^+	Lipid17[58] / ff99[50]	128	4480	303	2×600	2×100	72
DOPS/Na^+	Berger[24]	128	4480	303	2×500	2×100	73
DOPS/Na^+	GROMOS-CKPM*[64]	128	4480	303	2×500	2×100	74
DOPS/Na^+	GROMOS-CKP*[64]	128	4480	303	2×500	2×100	75
DOPS/Na^+	Slipids[67]	128	4480	303	2×500	2×100	76
DOPS/Na^+	Slipids[67]	288	11232	303	200	100	77

[a]Number of lipid molecules
[b]Number of water molecules
[c]Simulation temperature
[d]Total simulation time
[e]Time used for analyses
[f]Number of reference for simulation files

Table 2: List of POPC:POPS mixtures simulated at different molar fractions and different amounts of added $CaCl_2$. The salt concentrations are calculated as [salt]=N_c×[water] / N_w, where [water] = 55.5 M. This corresponds to the concentrations in buffer before solvating lipids, which were reported in the experiments by Roux et al.[17] Notation 2×[time] indicates that two independent MD runs were conducted. Dang refers to the ion parameters by Dang and co-workers,[78,79] and ff99 to the default Amber ion parameters.[50] The additional simulation details are given in the supplementary information. Symbols have the same meaning as in Table 1.

lipid/counter-ions	force field	[$CaCl_2$] (M)	N_l	N_w	[a]N_c	T (K)	t_{sim}(ns)	t_{anal} (ns)	files
POPC:POPS (5:1)/Na^+	CHARMM36[29,36]	0	110	4620	0	298	2×500	2×100	80
POPC:POPS (5:1)/K^+	CHARMM36[29,36]	0	110	4620	0	298	2×500	2×100	81
POPC:POPS (5:1)/K^+	CHARMM36[29,36]	0	250	11207	0	298	200	180	82
POPC:POPS (5:1)	CHARMM36[29,36] / NBfix1[35]	0.26	250	11190	53	298	200	180	83
POPC:POPS (5:1)	CHARMM36[29,36] / NBfix1[35]	1.06	250	11174	214	298	200	180	84
POPC:POPS (5:1)/Na^+	CHARMM36[29,36]	0	250	11207	0	320	400	300	85
POPC:POPS (5:1)/Na^+	CHARMM36[29,36] / NBfix2[86]	0.14	250	11190	28	320	440	300	85
POPC:POPS (5:1)/Na^+	CHARMM36[29,36] / NBfix2[86]	0.94	250	11174	189	320	440	300	85
POPC:POPS (1:1)/K^+	CHARMM36[29,36]	0	150	10785	0	298	200	180	87
POPC:POPS (1:0)	MacRog[55]	0	120	5120	0	298	200	150	88
POPC:POPS (5:1)/K^+	MacRog[55]	0	120	5760	0	298	400	250	89
POPC:POPS (5:1)/K^+	MacRog[55]	0.10	120	5760	10	298	600	300	89
POPC:POPS (5:1)/K^+	MacRog[55]	0.30	120	5760	31	298	600	300	89
POPC:POPS (5:1)/K^+	MacRog[55]	1.00	120	5760	104	298	600	300	89
POPC:POPS (5:1)/K^+	MacRog[55]	3.00	120	5760	311	298	600	300	89
POPC:POPS (5:1)/K^+	Lipid14/17[58,90] / ff99[50]	0	120	5760	0	298	2×500	2×200	91
POPC:POPS (5:1)/Na^+	Lipid14/17[58,90] / ff99[50]	0	120	5760	0	298	2×500	2×200	92
POPC:POPS (5:1)	Lipid14/17[58,90] / ff99[50]	0.50	120	5760	52	298	2×500	2×200	93
POPC:POPS (5:1)	Lipid14/17[58,90] / ff99[50]	1.00	120	5760	104	298	2×500	2×200	93
POPC:POPS (5:1)	Lipid14/17[58,90] / ff99[50]	2.00	120	5760	208	298	2×500	2×200	93
POPC:POPS (5:1)	Lipid14/17[58,90] / ff99[50]	3.00	120	5760	311	298	2×500	2×200	93
POPC:POPS (5:1)	Lipid14/17[58,90] / ff99[50]	4.00	120	5760	415	298	2×500	2×200	93
POPC:POPS (5:1)/Na^+	Lipid14/17[58,90] / Dang[78,79]	0	60	3600	0	298	1050	1000	94
POPC:POPS (5:1)/Na^+	Lipid14/17[58,90] / Dang[78,79]	0.08	60	3561	5	298	1050	1000	94
POPC:POPS (5:1)/Na^+	Lipid14/17[58,90] / Dang[78,79]	0.13	60	3561	8	298	1050	1000	94
POPC:POPS (5:1)/Na^+	Lipid14/17[58,90] / Dang[78,79]	0.20	60	3561	13	298	1050	1000	94
POPC:POPS (5:1)/Na^+	Lipid14/17[58,90] / Dang[78,79]	0.41	60	3522	26	298	1050	1000	94
POPC:POPS (5:1)/Na^+	Lipid14/17[58,90] / Dang[78,79]	0.62	60	3483	39	298	1050	1000	94
POPC:POPS (4:1)/Na^+	Berger[24,95]	0	102	4290	0	310	120	80	96
POPC:POPS (4:1)	Berger[24,95]	0.102[b]	104	4306	24	310	300	100	97
POPC:POPS (4:1)	Berger[24,95]	0.715[b]	104	4306	72	310	300	100	98
POPC:POPS (5:1)/Na^+	GROMOS-CKP[c 64]	0	110	4620	0	298	2×500	2×100	99
POPC:POPS (5:1)/Na^+	GROMOS-CKPM[c 64]	0	110	4620	0	298	2×500	2×100	100

[a]Number of Ca^{2+} cations in addition to counter ions

[b]Calculation of concetration complicated by the use of scaled ions. Concentration taken as reported in the delivered data.

[c]Force field parameters for PS lipids generated for this work, for full details see the supplementary information.

The ion number density profiles were calculated using the `gmx density` tool of the Gromacs sofware package.[104]

Using the molecular electrometer concept to compare ion binding to negatively charged lipid bilayers in simulations and in experiments

The S_{CH} of the α and β carbons in the PC headgroup decrease proportionally to the amount of positive charge bound to the bilayer,[105–107] and can therefore be used to measure the ion binding affinity. In addition to ions, the correlation between bound charge and headgroup order parameter change is empirically observed also for peptides, charged amphiphiles, local anesthetics and charged lipids.[43,108] This concept, known as the molecular electrometer, is especially useful for comparison between simulations and experiments, as the headgroup S_{CH} at varying cation concentrations can be easily calculated from simulations.[39] The headgroup S_{CH} of negatively charged PS and PG lipids also exhibit systematic — although less well understood —dependencies on the bound charge.[17,109–111] Therefore, measuring the PC headgroup S_{CH} from mixed (here PS:PC) bilayers[17,18,111] (see also SI section S2) provides a more straightforward way of characterizing the ion binding to negatively charged membranes.

Calibrating the PC S_{CH} response to a known amount of bound charge[39,112] is an important preliminary step for using the molecular electrometer. This can be done using experimental data from mixtures of PC and monovalent cationic surfactants (such as POPC and dihexadecyldimethylammonium, see SI section S3).[112,113] Additionally, the response of PC headgroup S_{CH} to the negatively charged PS follows the molecular electrometer in experiments,[43] which we also quantify here (see SI section S2).

Studies applying the molecular electrometer have used two different definitions for salt concentration: The concentrations can be reported either before,[17,39,105] or after[106,112] solvating the lipids. In the former case, binding of ions to the lipids leads to a lower bulk concentration

than in what was present in the original solvent. However, the choice of definition has only a marginal effect to the results in simulations with realistic ion binding affinity (see SI section S4). In this work we use the former definition (concentration before solvating the lipids) to be consistent with the reference experimental data.[17]

Results and Discussion

Headgroup and glycerol backbone C–H bond order parameters of POPS from ^{13}C NMR

The INEPT and 2D R-PDLF experiments from POPS samples gave well resolved spectra for all the carbons in the headgroup and glycerol backbone regions (Fig. 1). The glycerol backbone carbon peaks were assigned according to the POPC spectra,[46] whereas the peaks for β and α carbons were assigned according to the known C–H bond order parameters from the ^{2}H NMR experiments.[7] Slices of the R-PDLF spectra and the resulting S_{CH} values are shown in the supplementary information (Fig. S6).

Since the R-PDLF and previous ^{2}H NMR experiments[7,18] give only the absolute values of S_{CH}, we determined the signs of the PS headgroup S_{CH} using the S-DROSS experiment.[45] For a given carbon, its S-DROSS dipolar modulation profile in the indirect dimension is a superposition of sinusoidal functions from the possible orientations of crystallites in the sample (or bilayer patches). We phase corrected the 2D spectrum in the direct dimension such that positive and negative signs for the S_{CH} give rise to profiles that initially increase and decrease, respectively. In practice, we use the known negative sign of the acyl chain carbons as a reference to perform the phase correction and interpret the distinct initial slopes of the S-DROSS profiles (Fig. S6). The S-DROSS slice for the β-carbon clearly shows an initial decrease and therefore its order parameter must be negative. For the α-carbon such analysis is not as trivial due to the two inequivalent order parameters of the two distinct C–H bonds. However, the beginning of its S-DROSS slice suggests that the larger S_{CH} of

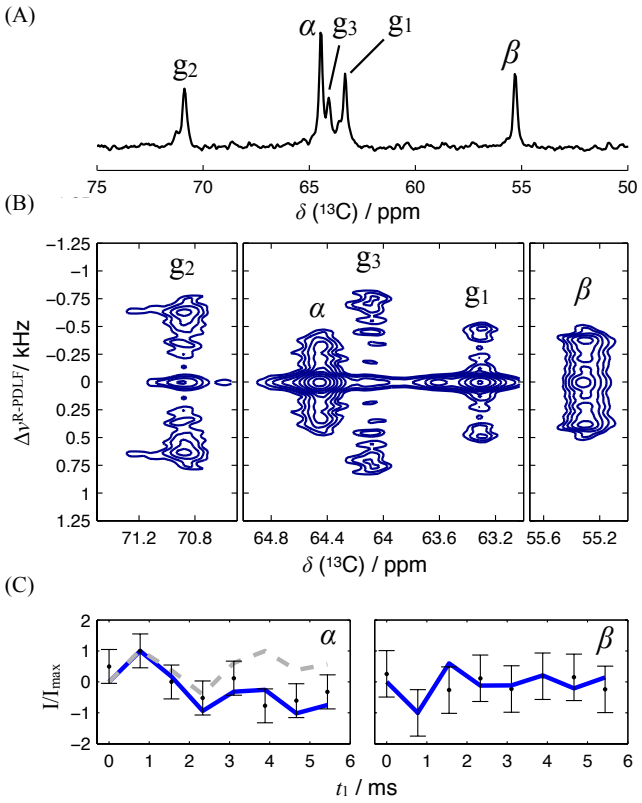

Figure 1: The headgroup and glycerol backbone region of the (A) Refocused-INEPT spectrum and (B) 2D R-PDLF spectra. (C) Experimental S-DROSS data (points), and SIMPSON simulations (blue lines) with the C–H bond order parameter values of −0.12 for the β-carbon, and +0.09 and −0.02 for the α-carbon. Dashed gray line is the S-DROSS curve from a SIMPSON simulation with a positive value (+0.02) for the smaller α-carbon C–H bond order parameter.

the α-carbon is positive and the decrease towards negative values at longer t_1 suggests that the smaller S_{CH} is negative. This is confirmed by a SIMPSON simulation using the S_{CH} values of +0.09 from the dipolar coupling measured here (Fig. S6) and −0.02 from the previous ^{2}H NMR experiment.[18] We used the literature value for the smaller S_{CH} , because the resolution of our R-PDLF experiment was not sufficient to determine the magnitude of the small value. The S-DROSS curve from the SIMPSON simulation with a positive value for the smaller S_{CH} (dashed grey in Fig. 1 C)) did not agree with the experiment, corroborating the interpretation that the smaller S_{CH} is negative.

The headgroup and glycerol backbone order parameters of POPS measured in this work are in good agreement with the previously reported values from ^{2}H NMR experiments of

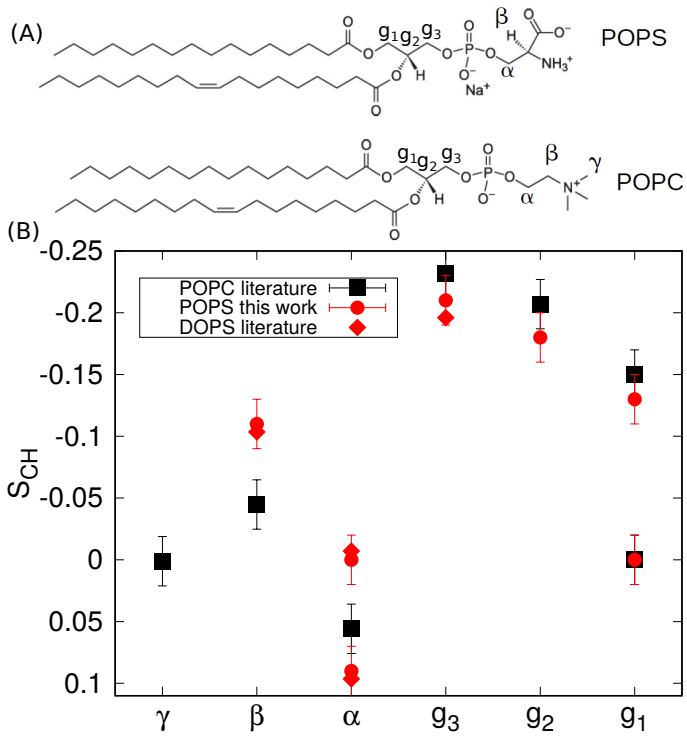

Figure 2: (A) Chemical structures and labels for the headgroup and glycerol backbone carbons. (B) Headgroup and glycerol backbone order parameters of POPS (T = 298 K) measured in this work compared with the previously published values from DOPS ($T = 303$ K, ^{2}H NMR, 0.1 M of NaCl)[7] and POPC ($T = 300$ K, ^{13}C NMR)[46] experiments. Signs of the PS order parameters are measured in this work whereas signs of the PC order parameters are measured previously.[47] The size of errorbars (± 0.02) shown for ^{13}C NMR data is justified previously.[38,40]

DOPS[7] (Fig. 2). When compared with the previously measured values for POPC[46] (Fig. 2), the β-carbon S_{CH} is significantly more negative and α-carbon experiences a substantial forking (different S_{CH} for the two hydrogens in the same carbon[40]) in the PS headgroup. These features have been intepreted to arise from a rigid PS headgroup conformation, stabilized by hydrogen bonds or electrostatic interactions,[7,8] but a detailed structrural interpretation is not available.

We note that the DOPS ^{2}H NMR reference data found in the literature[7,17] was obtained by first solvating the lipids with a buffer solution and then centrifuging the sample to a pellet that was used for the measurements. Such samples have a lower lipid concentration (approximately 10 wt % of lipids[7,17,114]) than the gravimetric samples (60 wt %) and sim-

ulations (approximately 50–60 wt %) in this work. Larger multilamellar repeat distances are expected in the samples with lower lipid concentrations due to the swelling caused by electrostatic repulsion in pure PS lipid systems.[115] Yet the PS headgroup S_{CH} measured from gravimetric samples (POPS) in this work are in good agreement with the results from centrifuged samples.[7] This, together with the rapid decrease of equilibrium repeat distance with addition of monovalent salt,[115,116] indicates that the hydration levels of multilamellae are sufficiently similar in the simulations and reference experiments.

Headgroup and glycerol backbone in simulations of PS lipid bilayers without additional ions

The different PS MD models produce highly varied headgroup and glycerol backbone S_{CH} (Fig. 3) and structures (Fig. S9 and section S6 in the supplementary information). As was previously observed for PC lipids,[38] also none of the PS models produces a set of S_{CH} in full quantitative agreement with the experiments. In fact, the models perform less well for PS than for PC (Figs. 3 and 5 vs. Figs. 2 and 4 in Ref.[38]), which complicates the interpretation of structural differences between the PC and PS. However, concentrating on the headgroup alone, we see that the best performing models (Slipids, CHARMM36 and CHARMM36-UA) indeed do replicate the larger-than-in-PC forking of the α-carbon that is observed in experiments (Fig. 3). Additionally, the Slipids force field correctly produces the significantly smaller β-carbon S_{CH} for PS compared to PC (Fig. 3 vs. Fig. 2 in Ref. 38), in line with experiments (Fig. 2).

Interestingly, in the three models that best fit the experimental data, the C_α-C_β-C_γ-O_γ dihedral angle distribution has a single peak around 120°, while other models yield binodal distributions (Fig. S7). The restricted motion is also visible in the sampled conformations (Figs. 4 (A) and S9), suggesting that the rotation of the carboxyl group is limited in the serine headgroup. On the other hand, the C_β-C_α-O_α-P dihedral angle rotates relatively freely between approximately 100° and 300° in the best three models (as seen also in Fig. 4 (B)),

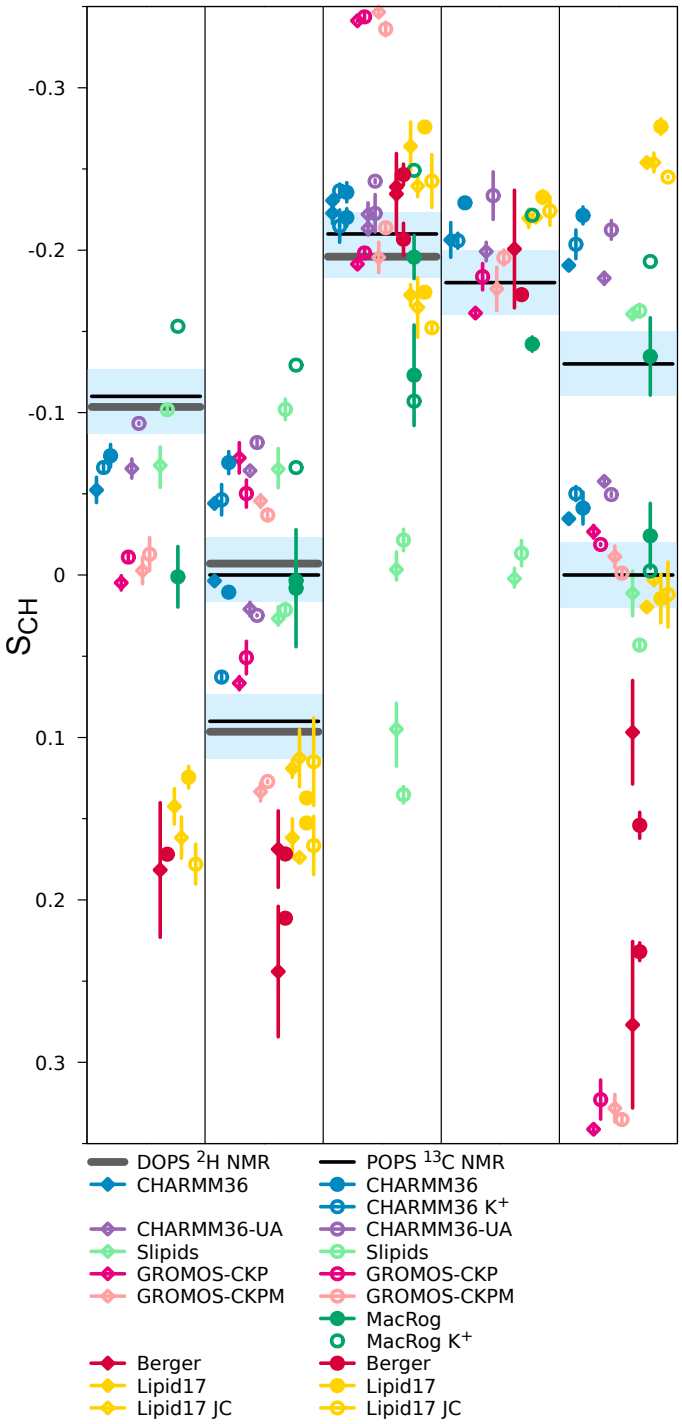

Figure 3: C–H bond order parameters, S_{CH}, of PS headgroup (β and α) and glycerol backbone (g_3, g_2, g_1) carbons from NMR experiments (horizontal lines), and MD simulations with different force fields (symbols). Experimental data for DOPS are measured with 0.1 M of NaCl,[7] while all the other data are with counterions only. The data for DOPS is at 303 K and for POPS at 298 K. Light blue areas span 0.04 units around the average of the extremal experimental values, in accordance with the expected quantitative accuracy of experiments.[40] The vertical bars shown for all simulation values (excl. MacRog K$^+$) are not error bars, but demonstrate that for these systems we had at least two data sets; the ends of the bars mark the extreme values from the sets, and the symbol marks their measurement-time-weighted average.

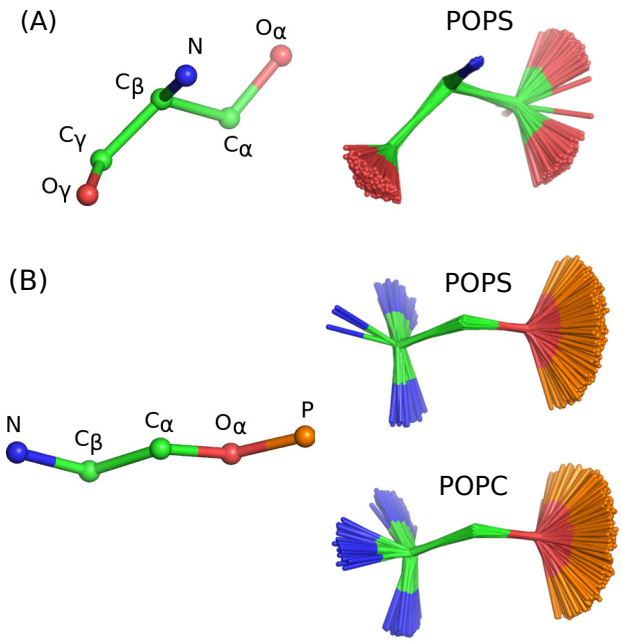

Figure 4: Overlayed snapshots from simulations conducted with CHARMM36—the force field producing the best agreement with experiments—demonstrate the conformational fluctuations of lipid headgroups. (A) Overlaying C_γ-C_β-C_α carbons demonstrate fluctuations around O_γ-C_γ-C_β-C_α, C_γ-C_β-C_α-O_α, and N-C_β-C_α-O_α dihedrals of the PS headgroup and (B) overlaying C_β-C_α-O_α carbonds demonstrate fluctuations around N-C_β-C_α-O_α and C_β-C_α-O_α-P dihedrals of the PS and PC headgroups. The trajectory used for CHARMM36 POPC is available at Ref. 117.

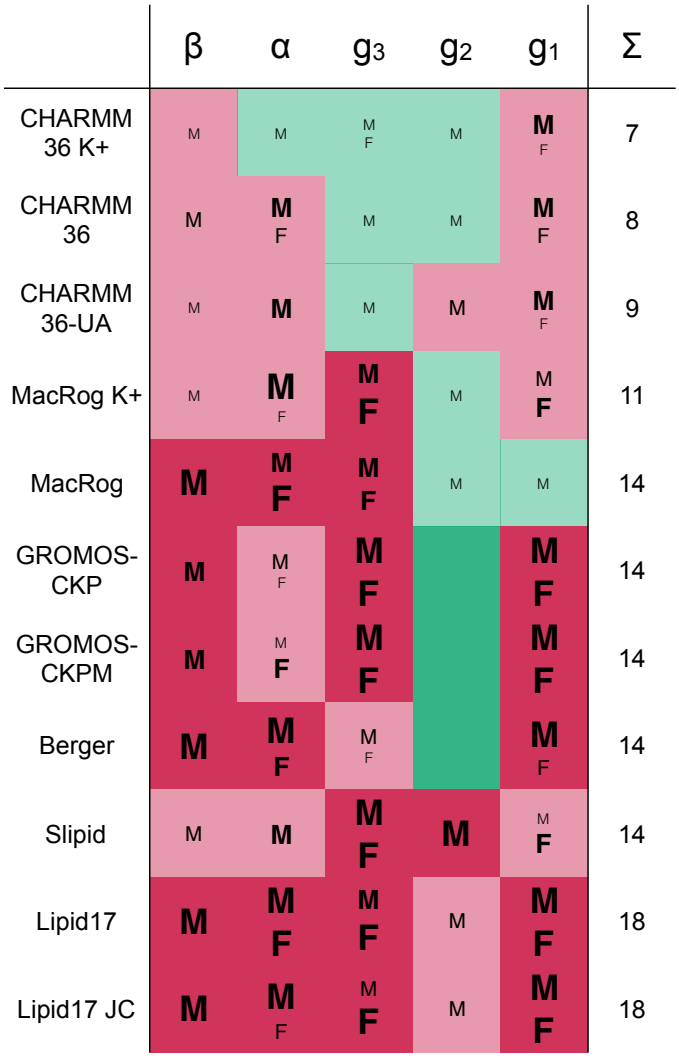

Figure 5: Rough subjective ranking of force fields based on how far are the simulated order parameters from the experimental values (M indicates a magnitude problem) and how well the difference between order parameters of the two hydrogens attached in the same carbon are reproduced (F indicates a forking problem) in Figure 3. The letter size increases with problem severity. Color scheme: "within experimental error" (dark green), "almost within experimental error" (light green), "clear deviation from experiments" (light red), and "major deviation from experiments" (dark red). The Σ-column shows the total deviation of the force field, when individual carbons are given weights of 0 (matches experiment), 1, 2, and 4 (major deviation). For full details of the assessment, see Supplementary Information.

while other models yield more restricted conformations (Fig. S7).

In simulations that have the best agreement with experiments (CHARMM36 and Slipids), the N-C_β-C_α-O_α dihedral exhibits a more asymmetric angle distribution for PS than for PC headgroup (Figs. 4 (B) and S10), which might reflect the increased rigidity proposed in the early experimental studies.[7,8] The suggested characteristic conformations of the PS headgroup can be useful when interpreting experiments, however, as the none of the tested models fully reproduces the experimental order parameters, more accurate MD force fields are required to elucidate the correct conformational ensemble.

Counterion binding and interactions between PC and PS headgroups

Membranes containing PS lipids are always accompanied with counterions that modulate electrostatic interactions between the lipids and other biomolecules. MD simulations have suggested that counterions reduce the area per lipid of PS bilayers compared to PC bilayers[23–25] by screening the repulsion between charged lipid headgroups. We explored this by quantifying the counterion density profiles along the membrane normal, accompanied by the areas per lipid, see Fig. 6. The force fields studied show significant differences in both binding affinity and distribution of ions at the interface. The experimental area per lipid (62.7 ± 1.3 Å^2)[30] is reproduced only in GROMOS-CKP and in the MacRog simulation with potassium counterions, while other models give considerably smaller values (Fig. 6). However, the counterion binding and the concomitant electrostatic screening of the headgroup repulsion does not fully explain the low area per molecule values since the MacRog simulation, which has the strongest sodium binding (the lowest concentrations in bulk water), gives the same area per molecule as the CHARMM36-UA simulation, which has significantly weaker counterion binding affinity. On the other hand, MacRog simulations with potassium produce a larger area per molecule (63 Å^2) than with sodium (53 Å^2) in line with the weaker potassium binding affinity (Fig. 6). The results are consistent with a previous study suggesting that the low areas per molecule

in PS lipid bilayers originate from the combination of both the counterion binding and intermolecular interactions between lipid headgroups.[118]

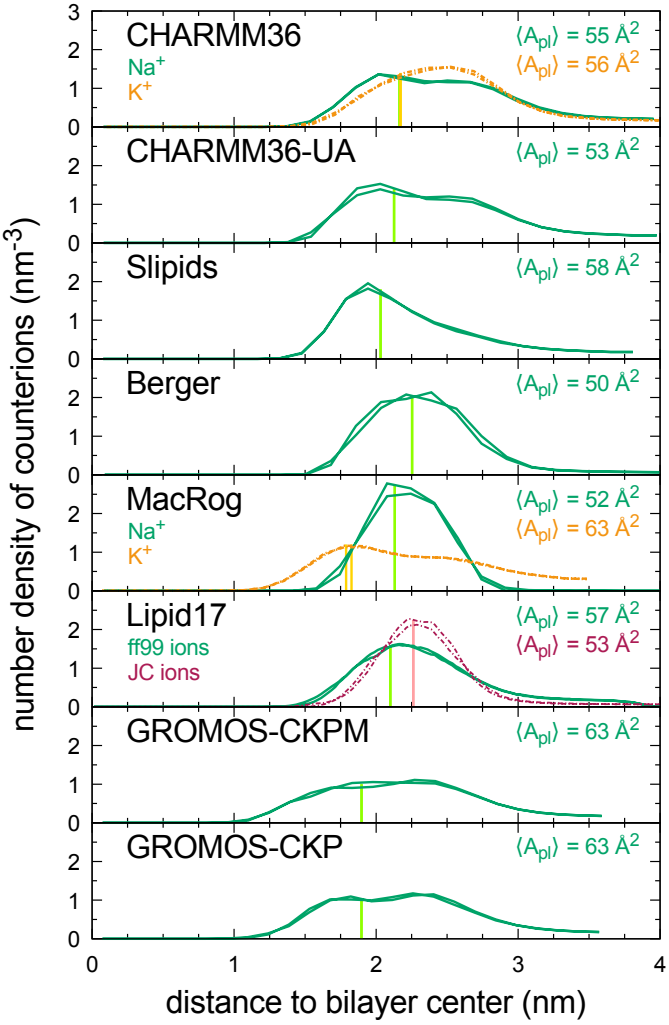

Figure 6: Counterion density profiles along the membrane normal and areas per lipid (A_{pl}) of POPS lipid bilayer from simulations with different force fields. The vertical green bars indicate the location of the phosphate density peak. The experimental area per lipid is 62.7 ± 1.3 Å^2.[30]

The experimentally observed modulation of headgroup order parameters by increasing salt concentration (the molecular electrometer concept) has been previously used to evaluate the cation binding to zwitterionic PC bilayers in simulations.[39] Studying binding of cations to negatively charged lipid bilayers is less straighforward due to the presence of cationic

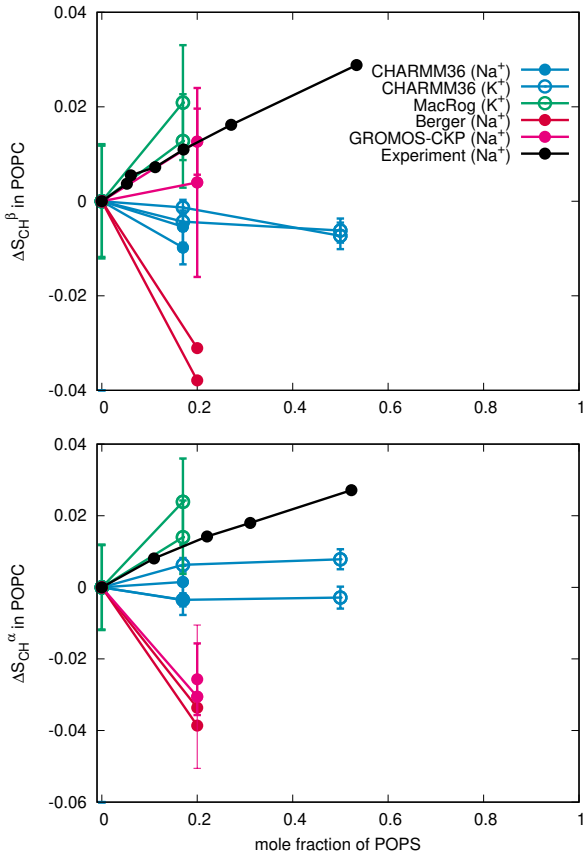

Figure 7: Changes of POPC headgroup order parameters with increasing amount of POPS in POPC:POPS mixtures at 298 K. Experimental values are from Ref. 43, with the signs measured in Ref. 47. The values from the CHARMM36 and GROMOS-CKP simulations with sodium are averages of two independent simulations and the error bar is given as the difference between the results divided by two.

counterions (the lack of an ion-free reference state). The analysis is further complicated by the artificial aggregation of counterions observed in some simulations (section S7 in the SI). Therefore, we evaluate here the amount of bound charge not by adding salt (although this is discussed in the SI section S7), but by studying the changes of the headgroup S_{CH} order parameters with increasing amount of negatively charged lipids (and thus increasing amount of cationic counterions) in the bilayer.

Experimentally, the S_{CH} values of the α and β headgroup carbons of POPC increase when negatively charged POPS lipids are incorporated in the bilayer (section S1).[43,107] This is reproduced in the MacRog simulations with potassium counterions (Fig. 7), which have

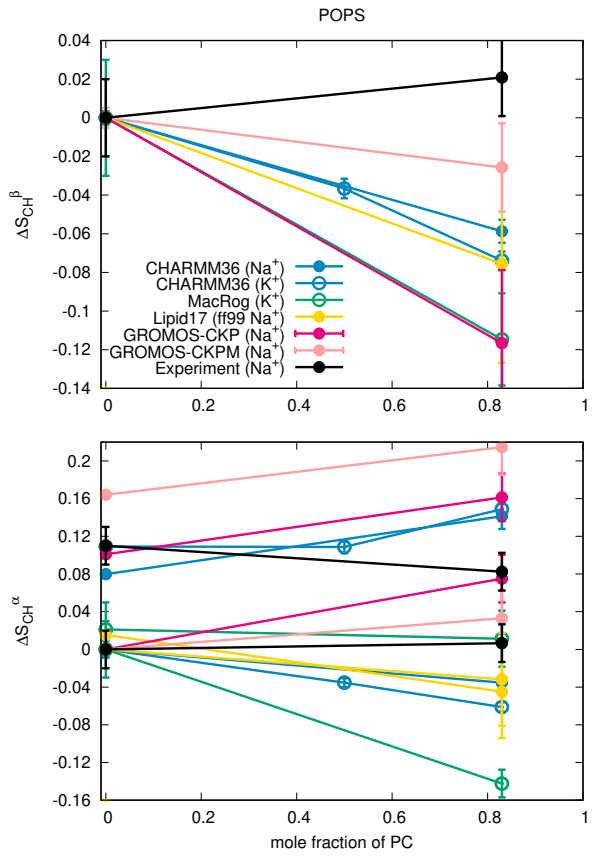

Figure 8: Modulation of POPS headgroup order parameters with increasing amount of POPC in POPC:POPS mixtures at 298 K. Experimental values with the signs are measured for pure POPS system in this work. The signs are assumed to be the same for the mixture and the values are from Ref. 17. Because the experimental values of POPS in pure and mixed bilayers come from ^{13}C NMR (this work) and ^{2}H NMR (Ref. 17), respectively, the error bars of 0.02 are used here.[38,40] The y-axis for the α-carbon results of POPS (bottom) is shifted with the same value for both order parameters such that the lower order parameter value from pure POPS is at zero to correctly illustrate the significant forking. The values from CHARMM36 and GROMOS simulations are averages of two independent simulations and the error bars are given as the difference between the results divided by two.

the weakest binding affinity to POPS lipid bilayers (Fig. 6). The CHARMM36, Berger and GROMOS-CKP simulations either exhibit no change or show a decrease in either or both the POPC headgroup order parameters as the amount of POPS increases (Fig. 7). Therein, the stronger counterion binding cancels the effect of negatively charged headgroups and prevents the experimentally observed increase of headgroup order parameters with growing amount of PS lipids. Therefore, we suggest that the relatively weak binding of potassium

in the MacRog simulations (Fig. 6) produces the most realistic surface charge density in membranes containing PS lipids, while the other tested models overestimate the counterion binding affinity. The results are consistent with the behavior of headgroup order parameters as a function of added counterions analyzed in section S7 in the SI.

The reduced forking of the POPS α-carbon (Fig. 8) together with other experimental results suggest that the PS headgroup structure becomes less rigid when diluted with POPC.[7,8,17,18,43] Unfortunately, none of the tested models correctly reproduce the modulation of POPS headgroup order parameters with increasing amount of POPC in POPC:POPS mixtures (Fig. 8). More accurate force fields are needed to correctly describe the PC–PS headgroup interactions in MD simulations.

Ca^{2+} binding affinity to bilayers with negatively charged PS lipids

Calcium binding affinity to membranes containing negatively charged PS lipids can be experimentally quantified by measuring the PC lipid headgroup order parameters from POPC:POPS (5:1) mixtures (section S2), where the measurement is not compromised by the dehydrated lipid–ion complexes and phase separation, and the bilayer remains uniform.[15–18] Despite the lack of an ion-free reference state in the presence of negatively charged lipids, our simulations give coherent results for POPC headgroup order parameters as a function of $CaCl_2$ in the POPC:POPS (5:1) mixtures (Fig. 9). As expected from the previous study of pure PC lipid bilayers,[39] almost all the tested simulation models overestimate the experimentally observed[17] decrease of the POPC headgroup order parameters upon increasing Ca^{2+} concentration (Fig. 9), indicating too strong calcium binding affinity. The sole exception is the CHARMM36 model when paired with the NBfix corrections for calcium.[35,86] For these combinations, the modulation of order parameters is underestimated, indicating a weaker binding affinity than in experiments. Notably, the CHARMM36 model together with the NBfix corrections[29,35] suggest similar binding affinities of calcium and sodium for a POPC bilayer (see section S8), in contrast to the experiments.[105,106,120] This suggests that the

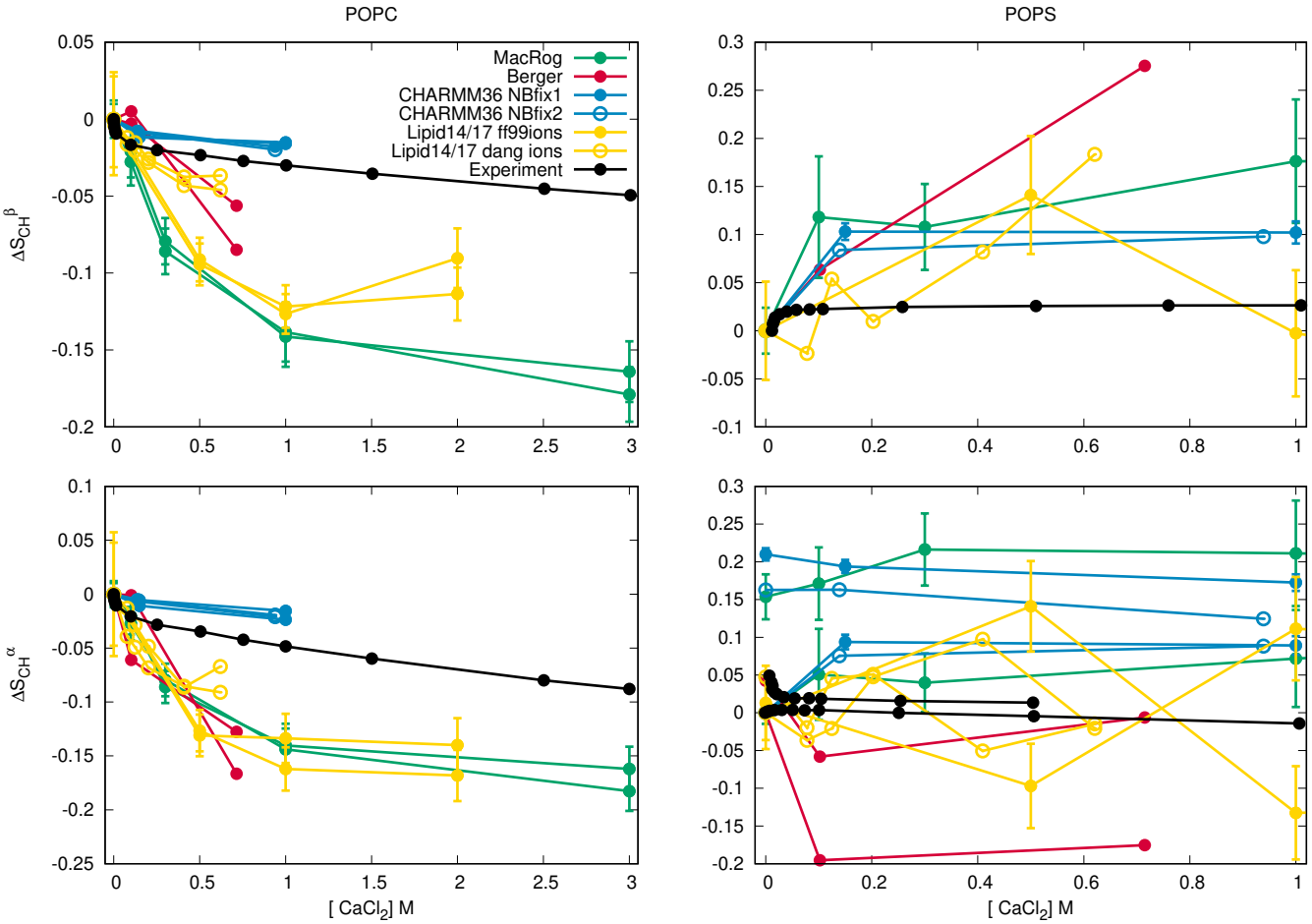

Figure 9: Variation of POPC (left) and POPS (right) headgroup order parameters from POPC:POPS (5:1) mixture as a function $CaCl_2$ concentration from experiments[17] and different simulations at 298 K (except the data for Berger model is from simulation of POPC:POPS (4:1) mixture at 310 K[32,119]). The order parameter values from systems without calcium are set as the zero point of y-axis, except for the α-carbon order parameter of POPS (bottom, right) for which both order parameters are shifted such that the lower order parameter is zero without additional ions. This is to correctly illustrate the forking with different concentrations of calcium. Potassium counterions are used in MacRog simulations and sodium counterions in Lipid14/17 simulations. In CHARMM36 and Berger simulation with added calcium, the charge is neutralized with calcium and monovalent counterions are not present.

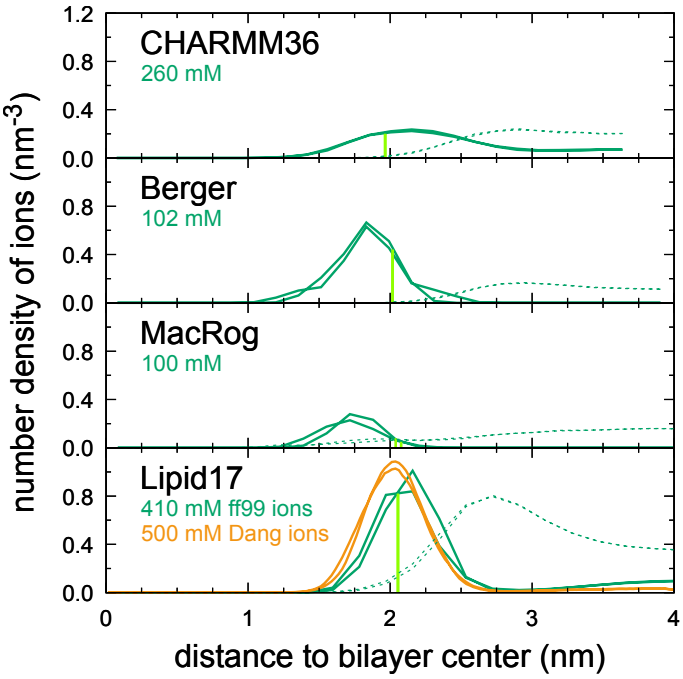

Figure 10: Number density profiles of Ca^{2+} (solid line) and Cl^- (dashed line) from POPC:POPS (5:1) mixtures simulated with different force fields. The vertical green bars indicate the location of the phosphate density peak. The smallest simulated $CaCl_2$ concentrations are shown. The density profiles for all the simulated concentrations are given in SI figure S18.

calcium binding affinity is underestimated in the CHARMM36 model when using the NBfix for calcium,[35,86] but overestimated in all the other tested models. This is evident in the calcium density distributions where almost all Ca^{2+} ions bind to the membrane interface in all simulation models except CHARMM36 (Fig. 10).

Experimentally, the POPS headgroup order parameters in POPC:POPS (5:1) mixtures exhibit a strong response to small concentrations of $CaCl_2$, which saturates below 100 mM (Fig. 9). The β-carbon order parameter increases with added $CaCl_2$, whereas the larger α-carbon order parameter decreases. Moreover, a slight increase is observed in the smaller α-carbon value. All these changes are significantly overestimated in the tested simulation models—including CHARMM36—which underestimated the binding affinity. Importantly, the different simulation models predict qualitatively different behavior for the two POPS α-carbon order parameters as a function of added calcium. For example, both order parameters

decrease in Berger, increase in MacRog, whereas Lipid14/17 and CHARMM36 models exhibit more complex behavior. This is in contrast to the PC headgroup, where a qualitatively correct response to bound ions is reproduced by all simulation models, despite the significant discrepancies in the headgroup structures observed in salt-free simulations.[39] The divergent response of the Berger model may arise from the ring like structures observed in the headgroup region in this model (Fig. 6 in Ref. 24). Therefore, we conclude that the improvement of force fields is necessary to correctly capture the interactions between the PS headgroup and calcium ions in MD simulations.

Conclusions

We used the headgroup C–H bond order parameters, S_{CH}, and the open collaboration approach to evaluate the quality of the headgroup structure and the ion binding affinity in available MD models of PS lipid. The main advantage of this approach is the direct connection between the order parameters measured accurately in experiments and calculated readily from simulations. This reduces the ambiguity in the interpretation of experiments.

First, we complemented the available experimental information[7,17] by measuring the signs of the PS headgroup order parameters, and then proceeded to compare MD simulation results from several force fields with the experimental data. This revealed that none of the force fields reproduce the PS headgroup order parameters within the experimental accuracy. However, the best models captured essential differences with PC and suggested characteristic conformations of PS headgroups. Comparison to the experimentally observed order parameters in POPC:POPS (5:1) bilayers at varying ion concentrations[17] then showed that the tested MD force fields overestimate the cation binding affinity to these bilayers with two exceptions: 1) the MacRog simulation with potassium counterions appears to produce the most realistic monovalent ion binding affinity to PS-containing lipid bilayers, and 2) the CHARMM36 force field with the recently introduced NBfix correction for calcium[35]

underestimates the calcium binding affinity. The experimentally measured response of the PS headgroup order parameters to the bound calcium, as well as to the dilution of bilayer with zwitterionic PC lipids, were not qualitatively reproduced in any of the tested force fields. This underlines the need for more accurate MD force fields to study the biological function of PS lipids. This is in contrast to the previous results with PC lipids, where the experimentally measured headgroup order parameter responses to the bound charge were in qualitative agreement even though the headgroup structures themselves were incorrect and the cation binding affinities were overestimated.[39]

We expect our results to pave the way for the development of better MD force fields for PS lipids. The quality of conformational ensembles produced by the various models can be evaluated based on the headgroup order parameters, which we hope to guide the development of force fields towards models that correctly reproduce the PS headgroup structures. Also, the ensembles observed in the simulations with the most realistic headgroup conformations (CHARMM36 and Slipids) hint the direction for the force field improvement. The cation binding can be improved based on the experimental headgroup order parameter data from POPC:POPS (5:1) mixtures under different cation concentrations. Recent studies showed that the cation binding to bilayers with POPC and POPS lipids can be improved by implicit inclusion of electronic polarizability using the electronic continuum correction (ECC),[112,121] suggesting that the electronic polarizability effects are important for lipid-ion interactions but polarizable force fields may not be necessary to correctly capture the ion binding to lipid bilayers.

Acknowledgement

MJ acknowledges financial support from the Emil Aaltonen foundation and and CSC-IT center for science for computational resources. JJM gratefully acknowledges financial support from the Carlsberg Foundation in the form of a postdoctoral fellowship while at

the University of Chicago (grants CF15-0552, CF16-0639, and CF17-0783) and the research framework provided by the Research Computing Center at the University of Chicago. OHSO acknowledges financial support from Academy of Finland (315596), Integrated Structural Biology Research Infrastructure of Helsinki Institute of Life Science (Instruct-HiLIFE), and CSC-IT center for science for computational resources. TJP wishes to acknowledge the use of the Iridis computing resources at the University of Southampton. FFR acknowledges Tecnológico Nacional de México Campus Zacatecas Occidente and Dirección General de Asuntos del Personal Académico (DGAPA) Programa de Apoyo a Proyectos de Investigación e Innovación Tecnológica (PAPIIT) IG100416 for financial support and Clúster Híbrido de Supercómputo Xiuhcoatl-CINVESTAV and Miztli-Dirección de Cómputo y de Tecnologías de Información y Comunicación (DGTIC)- Universidad Nacional Autónoma de México (UNAM) (Project LANCAD-UNAM-DGTIC-028) facilities for computing-time allocation.

References

(1) Lemmon, M. A. Membrane recognition by phospholipid-binding domains. *Nat. Rev. Mol. Cell Biol.* **2008**, *9*, 99–111.

(2) Leventis, P. A.; Grinstein, S. The Distribution and Function of Phosphatidylserine in Cellular Membranes. *Annu. Rev. Biophys.* **2010**, *39*, 407–427.

(3) Li, L.; Shi, X.; Guo, X.; Li, H.; Xu, C. Ionic protein-lipid interaction at the plasma membrane: what can the charge do? *Trends Biochem. Sci* **2014**, *39*, 130 – 140.

(4) Yeung, T.; Gilbert, G. E.; Shi, J.; Silvius, J.; Kapus, A.; Grinstein, S. Membrane Phosphatidylserine Regulates Surface Charge and Protein Localization. *Science* **2008**, *319*, 210–213.

(5) Zhao, H.; Tuominen, E. K. J.; Kinnunen, P. K. J. Formation of Amyloid Fibers Triggered by Phosphatidylserine-Containing Membranes. *Biochemistry* **2004**, *43*, 10302–10307.

(6) Gorbenko, G. P.; Kinnunen, P. K. The role of lipid-protein interactions in amyloid-type protein fibril formation. *Chem. Phys. Lipids* **2006**, *141*, 72 – 82.

(7) Browning, J. L.; Seelig, J. Bilayers of phosphatidylserine: a deuterium and phosphorus nuclear magnetic resonance study. *Biochemistry* **1980**, *19*, 1262–1270.

(8) Büldt, G.; Wohlgemuth, R. The headgroup conformation of phospholipids in membranes. *J. Membr. Biol.* **1981**, *58*, 81–100.

(9) Hauser, H.; Finer, E.; Darke, A. Crystalline anhydrous Ca-phosphatidylserine bilayers. *Biochem. Biophys. Res. Commun.* **1977**, *76*, 267 – 274.

(10) Kurland, R. J. Binding of Ca2+ and Mg2+ to phosphatidylserine vesicles: Different effects on P-31 NMR shifts and relaxation times. *Biochem. Biophys. Res. Commun.* **1979**, *88*, 927 – 932.

(11) Eisenberg, M.; Gresalfi, T.; Riccio, T.; McLaughlin, S. Adsorption of monovalent cations to bilayer membranes containing negative phospholipids. *Biochemistry* **1979**, *18*, 5213–5223.

(12) Hauser, H.; Shipley, G. G. Interactions of monovalent cations with phosphatidylserine bilayer membranes. *Biochemistry* **1983**, *22*, 2171–2178.

(13) Dluhy, R.; Cameron, D. G.; Mantsch, H. H.; Mendelsohn, R. Fourier transform infrared spectroscopic studies of the effect of calcium ions on phosphatidylserine. *Biochemistry* **1983**, *22*, 6318–6325.

(14) Hauser, H.; Shipley, G. Comparative structural aspects of cation binding to phosphatidylserine bilayers. *Biochim. Biophys. Acta* **1985**, *813*, 343 – 346.

(15) Feigenson, G. W. On the nature of calcium ion binding between phosphatidylserine lamellae. *Biochemistry* **1986**, *25*, 5819–5825.

(16) Mattai, J.; Hauser, H.; Demel, R. A.; Shipley, G. G. Interactions of metal ions with phosphatidylserine bilayer membranes: effect of hydrocarbon chain unsaturation. *Biochemistry* **1989**, *28*, 2322–2330.

(17) Roux, M.; Bloom, M. Calcium, magnesium, lithium, sodium, and potassium distributions in the headgroup region of binary membranes of phosphatidylcholine and phosphatidylserine as seen by deuterium NMR. *Biochemistry* **1990**, *29*, 7077–7089.

(18) Roux, M.; Bloom, M. Calcium binding by phosphatidylserine headgroups. Deuterium NMR study. *Biophys. J.* **1991**, *60*, 38 – 44.

(19) Boettcher, J. M.; Davis-Harrison, R. L.; Clay, M. C.; Nieuwkoop, A. J.; Ohkubo, Y. Z.; Tajkhorshid, E.; Morrissey, J. H.; Rienstra, C. M. Atomic View of Calcium-Induced Clustering of Phosphatidylserine in Mixed Lipid Bilayers. *Biochemistry* **2011**, *50*, 2264–2273.

(20) Seelig, J. Interaction of phospholipids with Ca2+ ions. On the role of the phospholipid head groups. *Cell Biol. Int. Rep.* **1990**, *14*, 353 – 360.

(21) Sinn, C. G.; Antonietti, M.; Dimova, R. Binding of calcium to phosphatidylcholine-phosphatidylserine membranes. *Colloids Surf., A* **2006**, *282-283*, 410 – 419.

(22) López Cascales, J. J.; García de la Torre, J.; Marrink, S. J.; Berendsen, H. J. C. Molecular dynamics simulation of a charged biological membrane. *J. Chem. Phys.* **1996**, *104*, 2713–2720.

(23) Pandit, S. A.; Berkowitz, M. L. Molecular Dynamics Simulation of Dipalmitoylphosphatidylserine Bilayer with Na+ Counterions. *Biophys. J.* **2002**, *82*, 1818 – 1827.

(24) Mukhopadhyay, P.; Monticelli, L.; Tieleman, D. P. Molecular Dynamics Simulation of a Palmitoyl-Oleoyl Phosphatidylserine Bilayer with Na+ Counterions and NaCl. *Biophys. J.* **2004**, *86*, 1601 – 1609.

(25) Pedersen, U. R.; Leidy, C.; Westh, P.; Peters, G. H. The effect of calcium on the properties of charged phospholipid bilayers. *Biochim. Biophys. Acta* **2006**, *1758*, 573 – 582.

(26) Vernier, P. T.; Ziegler, M. J.; Dimova, R. Calcium Binding and Head Group Dipole Angle in Phosphatidylserine-Phosphatidylcholine Bilayers. *Langmuir* **2009**, *25*, 1020–1027.

(27) Martín-Molina, A.; Rodríguez-Beas, C.; Faraudo, J. Effect of Calcium and Magnesium on Phosphatidylserine Membranes: Experiments and All-Atomic Simulations. *Biophys. J.* **2012**, *102*, 2095 – 2103.

(28) Jurkiewicz, P.; Cwiklik, L.; Vojtíšková, A.; Jungwirth, P.; Hof, M. Structure, dynamics, and hydration of POPC/POPS bilayers suspended in NaCl, KCl, and CsCl solutions. *Biochim. Biophys. Acta* **2012**, *1818*, 609 – 616.

(29) Venable, R. M.; Luo, Y.; Gawrisch, K.; Roux, B.; Pastor, R. W. Simulations of Anionic Lipid Membranes: Development of Interaction-Specific Ion Parameters and Validation Using NMR Data. *J. Phys. Chem. B* **2013**, *117*, 10183–10192.

(30) Pan, J.; Cheng, X.; Monticelli, L.; Heberle, F. A.; Kucerka, N.; Tieleman, D. P.; Katsaras, J. The molecular structure of a phosphatidylserine bilayer determined by scattering and molecular dynamics simulations. *Soft Matter* **2014**, *10*, 3716–3725.

(31) Vangaveti, S.; Travesset, A. Separation of the Stern and diffuse layer in coarse-grained models: The cases of phosphatidyl serine, phosphatidic acid, and PIP2 monolayers. *J. Chem. Phys.* **2014**, *141*, 245102.

(32) Melcrová, A.; Pokorna, S.; Pullanchery, S.; Kohagen, M.; Jurkiewicz, P.; Hof, M.; Jungwirth, P.; Cremer, P. S.; Cwiklik, L. The complex nature of calcium cation interactions with phospholipid bilayers. *Sci. Reports* **2016**, *6*, 38035.

(33) Valentine, M. L.; Cardenas, A. E.; Elber, R.; Baiz, C. R. Physiological Calcium Concentrations Slow Dynamics at the Lipid-Water Interface. *Biophys. J.* **2018**, *115*, 1541 – 1551.

(34) Hallock, M. J.; Greenwood, A. I.; Wang, Y.; Morrissey, J. H.; Tajkhorshid, E.; Rienstra, C. M.; Pogorelov, T. V. Calcium-Induced Lipid Nanocluster Structures: Sculpturing of the Plasma Membrane. *Biochemistry* **2018**, *57*, 6897–6905.

(35) Kim, S.; Patel, D. S.; Park, S.; Slusky, J.; Klauda, J. B.; Widmalm, G.; Im, W. Bilayer Properties of Lipid A from Various Gram-Negative Bacteria. *Biophys. J.* **2016**, *111*, 1750 – 1760.

(36) Klauda, J. B.; Venable, R. M.; Freites, J. A.; O'Connor, J. W.; Tobias, D. J.; Mondragon-Ramirez, C.; Vorobyov, I.; MacKerell Jr, A. D.; Pastor, R. W. Update of the CHARMM All-Atom Additive Force Field for Lipids: Validation on Six Lipid Types. *J. Phys. Chem. B* **2010**, *114*, 7830–7843.

(37) Berger, O.; Edholm, O.; Jähnig, F. Molecular dynamics simulations of a fluid bilayer of dipalmitoylphosphatidylcholine at full hydration, constant pressure, and constant temperature. *Biophys. J.* **1997**, *72*, 2002 – 2013.

(38) Botan, A.; Favela-Rosales, F.; Fuchs, P. F. J.; Javanainen, M.; Kanduč, M.; Kulig, W.; Lamberg, A.; Loison, C.; Lyubartsev, A.; Miettinen, M. S. et al. Toward Atomistic Resolution Structure of Phosphatidylcholine Headgroup and Glycerol Backbone at Different Ambient Conditions. *J. Phys. Chem. B* **2015**, *119*, 15075–15088.

(39) Catte, A.; Girych, M.; Javanainen, M.; Loison, C.; Melcr, J.; Miettinen, M. S.; Monticelli, L.; Maatta, J.; Oganesyan, V. S.; Ollila, O. H. S. et al. Molecular electrometer and binding of cations to phospholipid bilayers. *Phys. Chem. Chem. Phys.* **2016**, *18*, 32560–32569.

(40) Ollila, O. S.; Pabst, G. Atomistic resolution structure and dynamics of lipid bilayers in simulations and experiments. *Biochim. Biophys. Acta* **2016**, *1858*, 2512 – 2528.

(41) Piggot, T. J.; Allison, J. R.; Sessions, R. B.; Essex, J. W. On the Calculation of Acyl Chain Order Parameters from Lipid Simulations. *J. Chem. Theory Comput.* **2017**, *13*, 5683–5696.

(42) Gally, H. U.; Pluschke, G.; Overath, P.; Seelig, J. Structure of Escherichia coli membranes. Glycerol auxotrophs as a tool for the analysis of the phospholipid head-group region by deuterium magnetic resonance. *Biochemistry* **1981**, *20*, 1826–1831.

(43) Scherer, P.; Seelig, J. Structure and dynamics of the phosphatidylcholine and the phosphatidylethanolamine head group in L-M fibroblasts as studied by deuterium nuclear magnetic resonance. *EMBO J.* **1987**, *6*.

(44) Dvinskikh, S. V.; Zimmermann, H.; Maliniak, A.; Sandstrom, D. Measurements of motionally averaged heteronuclear dipolar couplings in MAS NMR using R-type recoupling. *J. Magn. Reson.* **2004**, *168*, 194–201.

(45) Gross, J. D.; Warschawski, D. E.; Griffin, R. G. Dipolar Recoupling in MAS NMR: A Probe for Segmental Order in Lipid Bilayers. *J. Am. Chem. Soc.* **1997**, *119*, 796–802.

(46) Ferreira, T. M.; Coreta-Gomes, F.; Ollila, O. H. S.; Moreno, M. J.; Vaz, W. L. C.; Topgaard, D. Cholesterol and POPC segmental order parameters in lipid membranes: solid state ^{1}H-^{13}C NMR and MD simulation studies. *Phys. Chem. Chem. Phys.* **2013**, *15*, 1976–1989.

(47) Ferreira, T. M.; Sood, R.; Bärenwald, R.; Carlström, G.; Topgaard, D.; Saalwächter, K.; Kinnunen, P. K. J.; Ollila, O. H. S. Acyl Chain Disorder and Azelaoyl Orientation in Lipid Membranes Containing Oxidized Lipids. *Langmuir* **2016**, *32*, 6524–6533.

(48) Bak, M.; Rasmussen, J. T.; Nielsen, N. C. SIMPSON: A General Simulation Program for Solid-State NMR Spectroscopy. *J. Magn. Res.* **2000**, *147*, 296 – 330.

(49) Joung, I. S.; Cheatham, T. E. Determination of Alkali and Halide Monovalent Ion Parameters for Use in Explicitly Solvated Biomolecular Simulations. *J. Phys. Chem. B* **2008**, *112*, 9020–9041.

(50) Åqvist, J. Ion-water interaction potentials derived from free energy perturbation simulations. *J. Phys. Chem.* **1990**, *94*, 8021–8024.

(51) Piggot, T. CHARMM36 POPS simulations (versions 1 and 2) 298 K 1.0 nm LJ switching. 2017; `https://doi.org/10.5281/zenodo.1129415`.

(52) Piggot, T. CHARMM36 POPS simulations (versions 1 and 2) 298 K 1.0 nm LJ switching with K ions. 2018; `https://doi.org/10.5281/zenodo.1182654`.

(53) Lee, S.; Tran, A.; Allsopp, M.; Lim, J. B.; Henin, J.; Klauda, J. B. CHARMM36 United Atom Chain Model for Lipids and Surfactants. *J. Phys. Chem. B* **2014**, *118*, 547–556.

(54) Piggot, T. CHARMM36-UA POPS simulations (versions 1 and 2) 298 K 1.0 nm LJ switching. 2017; `https://doi.org/10.5281/zenodo.1129458`.

(55) Maciejewski, A.; Pasenkiewicz-Gierula, M.; Cramariuc, O.; Vattulainen, I.; Róg, T. Refined OPLS All-Atom Force Field for Saturated Phosphatidylcholine Bilayers at Full Hydration. *J. Phys. Chem. B* **2014**, *118*, 4571–4581.

(56) Piggot, T. MacRog POPS simulations (versions 1 and 2) 298 K with corrected PO not OP tails. 2018; `https://doi.org/10.5281/zenodo.1283335`.

(57) Javanainen, M. Simulation of a POPS membrane with potassium counterions. 2018; `https://doi.org/10.5281/zenodo.1434990`.

(58) Gould, I.; Skjevik, A.; Dickson, C.; Madej, B.; Walker, R. Lipid17: A Comprehensive AMBER Force Field for the Simulation of Zwitterionic and Anionic Lipids. 2018; In preparation.

(59) Miettinen, M. S.; Kav, B. Molecular dynamics simulation trajectory of an anionic lipid bilayer: 100 mol% POPS with Na+ counterions using Joung-Cheatham Ions. 2018; `https://doi.org/10.5281/zenodo.1148495`.

(60) Miettinen, M. S.; Kav, B. Molecular dynamics simulation trajectory of an anionic lipid bilayer: 100 mol% POPS with Na+ counterions using ff99 ions. 2018; `https://doi.org/10.5281/zenodo.1134869`.

(61) Piggot, T. Berger POPS simulations (versions 1 and 2) 298 K 1.0 nm cut-off. 2017; `https://doi.org/10.5281/zenodo.1129425`.

(62) Chandrasekhar, I.; Kastenholz, M.; Lins, R.; Oostenbrink, C.; Schuler, L.; Tieleman, D.; Gunsteren, W. A consistent potential energy parameter set for lipids: dipalmitoylphosphatidylcholine as a benchmark of the GROMOS96 45A3 force field. *Eur. Biophys. J.* **2003**, *32*, 67–77.

(63) Kukol, A. Lipid Models for United-Atom Molecular Dynamics Simulations of Proteins. *J. Chem. Theory Comput.* **2009**, *5*, 615–626.

(64) Piggot, T. J.; Piñeiro, Á.; Khalid, S. Molecular Dynamics Simulations of Phosphatidylcholine Membranes: A Comparative Force Field Study. *J. Chem. Theory Comput.* **2012**, *8*, 4593–4609.

(65) Piggot, T. GROMOS-CKP POPS simulations (versions 1 and 2) 298 K with Berger/Chiu NH3 charges and PME. 2017; `https://doi.org/10.5281/zenodo.1129431`.

(66) Piggot, T. GROMOS-CKP POPS simulations (versions 1 and 2) 298 K with GROMOS NH3 charges and PME. 2017; https://doi.org/10.5281/zenodo.1129435.

(67) Jämbeck, J. P. M.; Lyubartsev, A. P. Implicit inclusion of atomic polarization in modeling of partitioning between water and lipid bilayers. *Phys. Chem. Chem. Phys.* **2013**, *15*, 4677–4686.

(68) Piggot, T. Slipids POPS simulations (versions 1 and 2) 298 K 1.0 nm cut-off with LJ-PME. 2017; https://doi.org/10.5281/zenodo.1129441.

(69) Piggot, T. CHARMM36 DOPS simulations (versions 1 and 2) 303 K 1.0 nm LJ switching. 2017; https://doi.org/10.5281/zenodo.1129411.

(70) Piggot, T. CHARMM36-UA DOPS simulations (versions 1 and 2) 303 K 1.0 nm LJ switching. 2017; https://doi.org/10.5281/zenodo.1129456.

(71) Kav, B.; Miettinen, M. S. Molecular dynamics simulation trajectory of an anionic lipid bilayer: 100 mol% DOPS with Na+ counterions using Joung-Cheetham Ions. 2018; https://doi.org/10.5281/zenodo.1134871.

(72) Kav, B.; Miettinen, M. S. Molecular dynamics simulation trajectory of an anionic lipid bilayer: 100 mol% DOPS with Na+ counterions using ff99 Ions. 2018; https://doi.org/10.5281/zenodo.1135142.

(73) Piggot, T. Berger DOPS simulations (versions 1 and 2) 303 K 1.0 nm cut-off. 2017; https://doi.org/10.5281/zenodo.1129419.

(74) Piggot, T. GROMOS-CKP DOPS simulations (versions 1 and 2) 303 K with Berger/Chiu NH3 charges and PME. 2017; https://doi.org/10.5281/zenodo.1129429.

(75) Piggot, T. GROMOS-CKP DOPS simulations (versions 1 and 2) 303 K with GROMOS NH3 charges and PME. 2017; https://doi.org/10.5281/zenodo.1129447.

(76) Piggot, T. Slipids DOPS simulations (versions 1 and 2) 303 K 1.0 nm cut-off with LJ-PME. 2017; https://doi.org/10.5281/zenodo.1129439.

(77) Favela-Rosales, F. MD simulation trajectory of a fully hydrated DOPS bilayer: SLIPIDS, Gromacs 5.0.4. 2017. 2017; https://doi.org/10.5281/zenodo.495510.

(78) Smith, D. E.; Dang, L. X. Computer simulations of NaCl association in polarizable water. *J. Chem. Phys* **1994**, *100*, 3757–3766.

(79) Dang, L. X.; Schenter, G. K.; Glezakou, V.-A.; Fulton, J. L. Molecular simulation analysis and X-ray absorption measurement of Ca2+, K+ and Cl- ions in solution. *J. Phys. Chem. B* **2006**, *110*, 23644–54.

(80) Piggot, T. CHARMM36 POPS/POPC simulations (versions 1 and 2) 298 K 1.0 nm LJ switching with Na ions. 2018; https://doi.org/10.5281/zenodo.1182665.

(81) Piggot, T. CHARMM36 POPS/POPC simulations (versions 1 and 2) 298 K 1.0 nm LJ switching with K ions. 2018; https://doi.org/10.5281/zenodo.1182658.

(82) Madsen, J. J. MD simulations of bilayers containing PC/PS mixtures and CaCl_2: 250POPC_50POPS_neutral. 2019; https://doi.org/10.5281/zenodo.2542151.

(83) Madsen, J. J. MD simulations of bilayers containing PC/PS mixtures and CaCl_2: 250POPC_50POPS_0.15MCaCl_2. 2019; https://doi.org/10.5281/zenodo.2542176.

(84) Madsen, J. J. MD simulations of bilayers containing PC/PS mixtures and CaCl_2: 250POPC_50POPS_1MCaCl_2. 2019; https://doi.org/10.5281/zenodo.2542135.

(85) Nencini, R. PC/PS 5:1 bilayer, Na contraions, additional CaC_2, CHARMM36 FF, NBFIX-Han. 2019; http://doi.org/10.5281/zenodo.3371327.

(86) Han, K.; Venable, R. M.; Bryant, A.-M.; Legacy, C. J.; Shen, R.; Li, H.; Roux, B.; Gericke, A.; Pastor, R. W. Graph–Theoretic Analysis of Monomethyl Phosphate Clustering in Ionic Solutions. *The Journal of Physical Chemistry B* **2018**, *122*, 1484–1494.

(87) Madsen, J. J. MD simulations of bilayers containing PC/PS mixtures and CaCl_2: 150POPC_150POPS_neutral. 2019; `https://doi.org/10.5281/zenodo.2542164`.

(88) Javanainen, M. Simulation of a POPC bilayer at 298K, lipid model by Maciejewski and Rog. 2018; `https://doi.org/10.5281/zenodo.1167532`.

(89) Javanainen, M. Simulations of POPC/POPS membranes with CaCl_2. 2017; `https://doi.org/10.5281/zenodo.1409551`.

(90) Dickson, C. J.; Madej, B. D.; Skjevik, A. A.; Betz, R. M.; Teigen, K.; Gould, I. R.; Walker, R. C. Lipid14: The Amber Lipid Force Field. *J. Chem. Theory Comput.* **2014**, *10*, 865–879.

(91) Kav, B.; Miettinen, M. S. Amber Lipid17 Simulations of POPC/POPS Membranes with KCl Counterions. 2018; `https://doi.org/10.5281/zenodo.1250969`.

(92) Kav, B.; Miettinen, M. S. Amber Lipid17 Simulations of POPC/POPS Membranes with NaCl Counterions. 2018; `https://doi.org/10.5281/zenodo.1250975`.

(93) Kav, B.; Miettinen, M. S. Amber Lipid17 Simulations of POPC/POPS Membranes with CaCl2. 2018; `https://doi.org/10.5281/zenodo.1438848`.

(94) Melcr, J. Molecular dynamics simulations of lipid bilayers containing POPC and POPS with the lipid17 force field, only counterions, and CaCl2 concentrations. 2018; `https://doi.org/10.5281/zenodo.1487761`.

(95) Tieleman, D. P.; Berendsen, H. J.; Sansom, M. S. An Alamethicin Channel in a Lipid Bilayer: Molecular Dynamics Simulations. *Biophys. J.* **1999**, *76*, 1757 – 1769.

(96) Ollila, O. H. S. POPC:POPS (4:1) simulation with Berger model at 310K. 2018; https://doi.org/10.5281/zenodo.1475285.

(97) Cwiklik, L. MD simulation trajectory of a POPC/POPS (4:1) bilayer with 102mM CaCl2, Berger force field for lipids, scaled charges for Ca2+ and Cl-. 2017; https://doi.org/10.5281/zenodo.887398.

(98) Cwiklik, L. MD simulation trajectory of a POPC/POPS (4:1) bilayer with 715mM CaCl2, Berger force field for lipids, scaled charges for Ca2+ and Cl-. 2017; https://doi.org/10.5281/zenodo.887400.

(99) Piggot, T. GROMOS-CKP POPS/POPC simulations (versions 1 and 2) 298 K with GROMOS NH3 charges and PME. 2018; https://doi.org/10.5281/zenodo.1283333.

(100) Piggot, T. GROMOS-CKP POPS/POPC simulations (versions 1 and 2) 298 K with Berger/Chiu NH3 charges and PME. 2018; https://doi.org/10.5281/zenodo.1283331.

(101) ohsOllila,; et al., MATCH GitHub repository. https://github.com/NMRLipids/MATCH.

(102) Michaud-Agrawal, N.; Denning, E. J.; Woolf, T. B.; Beckstein, O. MDAnalysis: A toolkit for the analysis of molecular dynamics simulations. *J. Comput. Chem.* **2011**, *32*, 2319–2327.

(103) Richard J. Gowers,; Max Linke,; Jonathan Barnoud,; Tyler J. E. Reddy,; Manuel N. Melo,; Sean L. Seyler,; Jan Domański,; David L. Dotson,; Sébastien Buchoux,; Ian M. Kenney, et al. MDAnalysis: A Python Package for the Rapid Analysis of Molecular Dynamics Simulations. Proceedings of the 15th Python in Science Conference. 2016; pp 98 – 105.

(104) Abraham, M.; van der Spoel, D.; Lindahl, E.; Hess, B.; the GROMACS development team, GROMACS user manual version 5.0.7. 2015.

(105) Akutsu, H.; Seelig, J. Interaction of metal ions with phosphatidylcholine bilayer membranes. *Biochemistry* **1981**, *20*, 7366–7373.

(106) Altenbach, C.; Seelig, J. Calcium binding to phosphatidylcholine bilayers as studied by deuterium magnetic resonance. Evidence for the formation of a calcium complex with two phospholipid molecules. *Biochemistry* **1984**, *23*, 3913–3920.

(107) Seelig, J.; MacDonald, P. M.; Scherer, P. G. Phospholipid head groups as sensors of electric charge in membranes. *Biochemistry* **1987**, *26*, 7535–7541.

(108) Beschiaschvili, G.; Seelig, J. Peptide binding to lipid membranes. Spectroscopic studies on the insertion of a cyclic somatostatin analog into phospholipid bilayers. *Biochimica et Biophysica Acta (BBA) - Biomembranes* **1991**, *1061*, 78 – 84.

(109) Borle, F.; Seelig, J. Ca2+ binding to phosphatidylglycerol bilayers as studied by differential scanning calorimetry and 2H- and 31P-nuclear magnetic resonance. *Chem. Phys. Lipids* **1985**, *36*, 263 – 283.

(110) Macdonald, P. M.; Seelig, J. Calcium binding to mixed phosphatidylglycerol-phosphatidylcholine bilayers as studied by deuterium nuclear magnetic resonance. *Biochemistry* **1987**, *26*, 1231–1240.

(111) Roux, M.; Neumann, J.-M. Deuterium NMR study of head-group deuterated phosphatidylserine in pure and binary phospholipid bilayers. *FEBS Letters* **1986**, *199*, 33–38.

(112) Melcr, J.; Martinez-Seara, H.; Nencini, R.; Kolafa, J.; Jungwirth, P.; Ollila, O. H. S. Accurate Binding of Sodium and Calcium to a POPC Bilayer by Effective Inclusion of Electronic Polarization. *J. Phys. Chem. B* **2018**, *122*, 4546–4557.

(113) Scherer, P. G.; Seelig, J. Electric charge effects on phospholipid headgroups. Phosphatidylcholine in mixtures with cationic and anionic amphiphiles. *Biochemistry* **1989**, *28*, 7720–7728.

(114) Roux, M.; Neumann, J.-M.; Bloom, M.; Devaux, P. F. 2H and 31P NMR study of pentalysine interaction with headgroup deuterated phosphatidylcholine and phosphatidylserine. *Eur. Biophys. J.* **1988**, *16*, 267–273.

(115) Loosley-Millman, M.; Rand, R.; Parsegian, V. Effects of monovalent ion binding and screening on measured electrostatic forces between charged phospholipid bilayers. *Biophys. J.* **1982**, *40*, 221 – 232.

(116) Rand, R.; Parsegian, V. Hydration forces between phospholipid bilayers. *Biochim. Biophys. Acta* **1989**, *988*, 351 – 376.

(117) Melcr, J. POPC lipid membrane, 303K, Charmm36 force field, simulation files and 200 ns trajectory for Gromacs MD simulation engine v5.1.2. 2016; `https://doi.org/10.5281/zenodo.153944`.

(118) Petrache, H. I.; Tristram-Nagle, S.; Gawrisch, K.; Harries, D.; Parsegian, V. A.; Nagle, J. F. Structure and Fluctuations of Charged Phosphatidylserine Bilayers in the Absence of Salt. *Biophys. J.* **2004**, *86*, 1574 – 1586.

(119) Ollila, S.; Hyvönen, M. T.; Vattulainen, I. Polyunsaturation in Lipid Membranes: Dynamic Properties and Lateral Pressure Profiles. *J. Phys. Chem. B* **2007**, *111*, 3139–3150.

(120) Cevc, G. Membrane electrostatics. *Biochim. Biophys. Acta* **1990**, *1031*, 311 – 382.

(121) Melcr, J.; Ferreira, T.; Jungwirth, P.; Ollila, O. H. S. Improved Cation Binding to Lipid Bilayer with Negatively Charged POPS by Effective Inclu-

sion of Electronic Polarization. https://github.com/ohsOllila/ecc_lipids/blob/master/Manuscript/manuscript.pdf, Submitted.